Journal of Power Sources 195 (2010) 829–833

Contents lists available at ScienceDirect

Journal of Power Sources

journal homepage: www.elsevier.com/locate/jpowsour

Short communication

Analysis of ammonia decomposition reactor to generate hydrogen for fuel cell applications

Vyjayanthi Alagharu, Srinivas Palanki*, Kevin N. West

Department of Chemical & Biomolecular Engineering, University of South Alabama, 307 University Blvd N., Mobile, AL 36688-0002, USA

ARTICLE INFO

Article history:
Received 9 July 2009
Received in revised form 3 August 2009
Accepted 8 August 2009
Available online 19 August 2009

Keywords:
Ammonia decomposition
Hydrogen generation
Fuel cell

ABSTRACT

In this paper, reaction engineering principles are utilized to analyze process conditions for producing sufficient hydrogen in an ammonia decomposition reactor for generating net power of 100 W in a fuel cell. It is shown that operating the reactor adiabatically results in a sharp decrease in temperature due to endothermic reaction, which results in low conversion of ammonia. For this reason, the reactor is heated electrically to provide heat for the endothermic reactions. It is observed that when the reactor is operated non-adiabatically, it is possible to get over 99.5% conversion of ammonia. The weight of absorbent to reduce ammonia to *ppb* levels is calculated. An energy balance on the reactor exit gas indicates that there is sufficient heat available to vaporize enough water to achieve 100% relative humidity in the fuel cell. A suitable fuel cell stack is designed and it is shown that this stack is able to provide the necessary power to electrically heat the reactor and produce net power of 100 W.

1. Introduction

There is current interest in the development of technologies that provide alternatives to conventional batteries in the 100 W range to power portable devices in remote areas, where access to the power grid is limited. In particular, the development of power systems based on polymer electrolyte membrane (PEM) fuel cells that utilize hydrogen to produce power can provide thermodynamic and environmental advantages [1]. Fuel cells can operate for longer durations as compared to batteries and are only limited by the size of the fuel tank for generating power continuously. While the ultimate goal is to use renewable resources to generate hydrogen for use in a fuel cell stack to produce power, there are currently many barriers to the hydrogen economy because the issue of efficient storage and transport of hydrogen is not yet resolved. For this reason, there is considerable interest in utilizing fuel processing technologies to generate hydrogen *in situ* on an "as needed" basis. Fuel processing technologies convert a hydrogen containing material into a hydrogen rich stream [2]. One popular fuel processing technology involves steam reforming of hydrocarbons and there is a considerable amount of literature in this area that describes the fabrication of small reactors for mobile power applications. Pattekar and Kothare [3] fabricated a radial flow micro-packed-bed reactor via deep reactive ion etching that utilizes methanol to generate sufficient hydrogen for a 20 W power application. Sohn et al. [4] developed a plate-type integrated fuel processor-PEM fuel cell where methanol is reformed to produce up to 150 W of power. Tan et al. [5] developed a methane processing system for producing high-purity hydrogen for 10–1500 W power applications. Lindstrom et al. [6] developed a diesel fuel reformer for generating hydrogen for an auxiliary power unit in a truck. Chu et al. [7] developed a compact reformer that utilizes natural gas or propane to deliver up to 3 kW of power. Kolb et al. [8] developed a microstructure reactor that uses iso-octane as a hydrocarbon source for producing hydrogen for mobile auxiliary power units. A review of reformers that convert hydrocarbon fuel to hydrogen for fuel cell applications is available in Kundu et al. [9].

The use of hydrocarbons for producing hydrogen typically leads to the production of carbon monoxide, which poisons the PEM fuel cell catalyst. Furthermore, sulfur compounds in the hydrocarbons also present operational difficulties in the fuel cell. To alleviate these problems, it is necessary to add multiple processing steps such as water–gas shift reactions, methanation, oxidation and desulfurization. A viable alternative is to use ammonia as a source of hydrogen. Pure ammonia has an energy density of 8.9 kWh kg^{-1}, which is higher than methanol (6.2 kWh kg^{-1}), but less than diesel or JP-8 (13.2 kWh kg^{-1}) [10]. It is an inexpensive fuel that has an extensive distribution system [2]. Ammonia decomposition to hydrogen occurs in a single reaction step and there is no carbon monoxide or sulfur in the product stream. It has a strong odor, which makes leak detection simple [11]. Powell et al. [12] fabricated an integrated 50 W, 100 Wh ammonia cracker-PEM fuel cell prototype. While the potential for using ammonia as a hydrogen carrier has been recognized and small-scale reactors have been

* Corresponding author. Tel.: +1 251 460 6160; fax: +1 251 461 1485.
E-mail address: spalanki@usouthal.edu (S. Palanki).

0378-7753/$ – see front matter © 2009 Elsevier B.V. All rights reserved.
doi:10.1016/j.jpowsour.2009.08.024

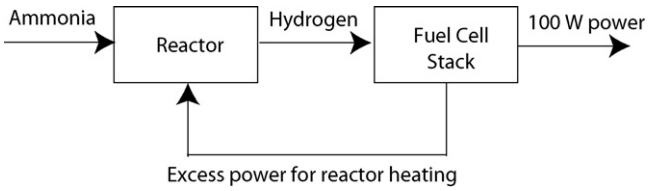

Fig. 1. Schematic of reformer and fuel cell system.

fabricated, the literature is very sparse in the area of modeling and analysis of reactors that utilize ammonia to produce hydrogen for fuel cell applications. In this paper, a packed-bed reactor is analyzed in which decomposition of ammonia occurs to produce hydrogen. In particular, the reactor is modeled as a non-isothermal, non-isobaric packed-bed reactor. The reactor is heated electrically Reactor conditions are analyzed to generate sufficient hydrogen that can be used in a polymer electrolyte (PEM) fuel cell to produce sufficient power to heat the reactor and a net usable power of 100 W. A schematic of the process under consideration is shown in Fig. 1.

2. Reactor modeling and simulation

Ammonia decomposition to produce hydrogen can be represented by the following equation [13]:

$$NH_3 \rightarrow 1.5H_2 + 0.5N_2 \tag{1}$$

This reaction is carried out in a temperature range of 793–853 K and a pressure range of 1–2 bar using a Ni-Pt catalyst. This reaction is endothermic with a heat of reaction of 46 kJ mol^{-1} of ammonia. In the temperature range stated above, the reaction is irreversible and the reaction rate is represented as follows [13]:

$$r_{NH_3} = k_0 \exp\left(-\frac{E}{RT}\right) p_{NH_3} \tag{2}$$

where r_{NH_3} is the reaction rate for decomposition of ammonia, k_0 is the frequency factor, E is the activation energy, R is the universal gas constant, T is the temperature, and p_{NH_3} is the partial pressure of ammonia.

The reformer is modeled as a packed-bed tubular reactor. The steady-state model equations for each species are given as follows [14]:

$$\frac{dF_{NH_3}}{dV} = -r_{NH_3} \tag{3}$$

$$\frac{dF_{H_2}}{dV} = 1.5r_{NH_3} \tag{4}$$

$$\frac{dF_{N_2}}{dz} = 0.5r_{NH_3} \tag{5}$$

where F_{NH_3}, F_{H_2}, and F_{N_2} are the molar flow rates of ammonia, hydrogen and nitrogen, respectively, and V is the volume dimension of the tubular reactor. The pressure drop is modeled via the Ergun equation [14]:

$$\frac{dP}{dV} = -\frac{G}{\rho D_p A_c}\left(\frac{1-\phi}{\phi^3}\right)\left[\frac{150(1-\phi)\eta_m}{D_p} + 1.75G\right] \tag{6}$$

where P is the reactor pressure, ϕ is the void fraction, D_p is the diameter of the catalyst particle in the reactor, η_m is the viscosity of the gas mixture, ρ is the gas mixture density, A_c is the cross-sectional area of the reactor and G is the superficial mass velocity.

The Ergun equation requires the computation of the gas mixture density, ρ, as well as the gas mixture viscosity, η_m, as a function of reactor volume. The mixture density is estimated by computing the mole average density of the gas mixture at each integration step. However, the mole average method can lead to significant errors in the computation of overall gas mixture viscosity due to the presence of hydrogen in the gas mixture [15]. For this reason, Wilke's method [16] is utilized to estimate the gas viscosity at each integration step as shown below:

$$\eta_m = \sum_{i=1}^{n} \frac{y_i \eta_i}{\sum_{j=1}^{n} y_j \phi_{ij}} \tag{7}$$

where

$$\phi_{ij} = \frac{[1 + (\eta_i/\eta_j)^{0.5}(M_j/M_i)^{0.25}]^2}{[8(1 + (M_i/M_j))]^{0.5}} \tag{8}$$

In the above equations, η_m is the viscosity of the mixture, η_i, y_i, and M_i are the viscosity, mole fraction and molecular weight of pure component i. The pure component viscosity is calculated by the following equation:

$$\eta_i = \frac{(26.69MT)^{0.5}}{\sigma^2 \Omega} \tag{9}$$

where σ is the hard spehere diameter, Ω is the collision integral and T is the temperature. Hard sphere diameters are obtained from Poling et al. [16] and the collision integral is calculated by the following equation:

$$\Omega = \frac{a}{\bar{T}^b} + \frac{c}{e^{\bar{T}d}} + \frac{e}{e^{\bar{T}f}} \tag{10}$$

where $\bar{T}$ is the dimensionless temperature given by (T/E_k) and E_k is the minimum of pair potential energy divided by Boltzmann constant and a, b, c, d, e are collision integral constants. Minimum of pair potential energy is obtained from Poling et al. [16]. Dimensionless temperature is used to determine the collision integral by means of collision integral constants.

A steady-state energy balance on the reformer leads to the following equation [14]:

$$\frac{dT}{dz} = \frac{Q + r_{NH_3}\Delta H}{F_{NH_3}C_{p_{NH_3}} + F_{N_2}C_{p_{N_2}} + F_{H_2}C_{p_{H_2}}} A_c \tag{11}$$

where T is the reformer temperature, ΔH is the heat of reaction, Q is the heat flux to the reactor that is provided via electrical heating, and C_{p_j} is the specific heat of species j.

Table 1 lists the kinetic parameters and reactor parameters used in simulation studies. Tables 2 and 3 list the parameters used for estimating gas viscosity via Wilke's method. The model neglects the reverse reaction. To support this assumption, the equilibrium constant was calculated as a function of standard state ΔG, ΔH and temperature dependent heat capacities. Fig. 2 shows plot of equilibrium constant as a function of temperature and it is observed that

Table 1
Kinetic and reactor parameters.

Parameter	Value
Frequency factor, k_0	1.33×10^{11} mol m^{-3} s^{-1} Pa^{-1}
Activation energy, E	1.9×10^5 J mol^{-1}
Catalyst particle diameter, D_p	0.00035 m
Catalyst density, ρ	2000 kg m^{-3}
Void fraction, ϕ	0.3
Reactor length, L	0.31 m
Reactor diameter, D_i	0.05 m
Specific heat of ammonia, $C_{p_{NH_3}}$	$19.99 + 49.77T - 15.37T^2 + 1.92T^3 + 0.18/T^2$ kJ kmol^{-1} K^{-1}
Specific heat of hydrogen, $C_{p_{H_2}}$	$26.09 + 8.21T - 1.97T^2 + 0.159T^3 + 0.04/T^2$ kJ kmol^{-1} K^{-1}
Specific heat of nitrogen, $C_{p_{N_2}}$	$33.06 - 11.36T + 11.43T^2 - 2.77T^3 - 0.15/T^2$ kJ kmol^{-1} K^{-1}

Table 2
Hard sphere diameters and potential energy.

Component	Hard sphere diameter (Å)	(Potential energy)/(Boltzmann constant) (K)
Ammonia	3.798	558.3
Hydrogen	2.900	59.7
Nitrogen	2.827	71.4

Table 3
Collision integral constants.

Collision integral constant	Value
a	1.16145
b	0.14874
c	0.52487
d	0.77320
e	2.16178
f	2.43787

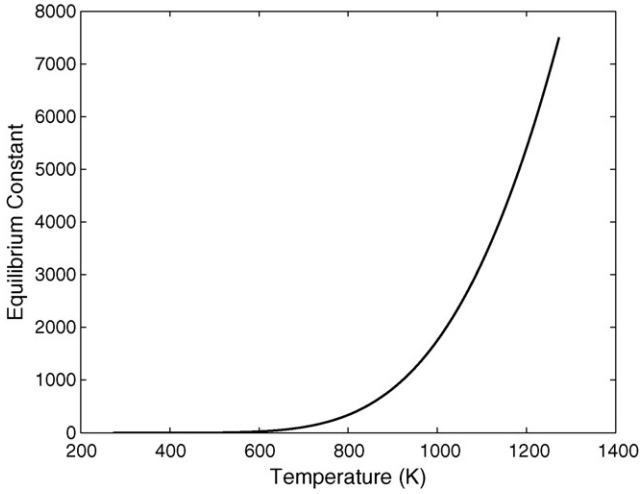

Fig. 2. Equilibrium constant as a function of temperature.

in the temperature range of 800–870 K, the equilibrium constant is in the range of 350–670. Fig. 3 shows the plot of equilibrium conversion as a function of temperature at an outlet pressure of 1.9 bar. It is observed that the equilibrium conversion is greater than 99.5% for temperatures higher than 800 K.

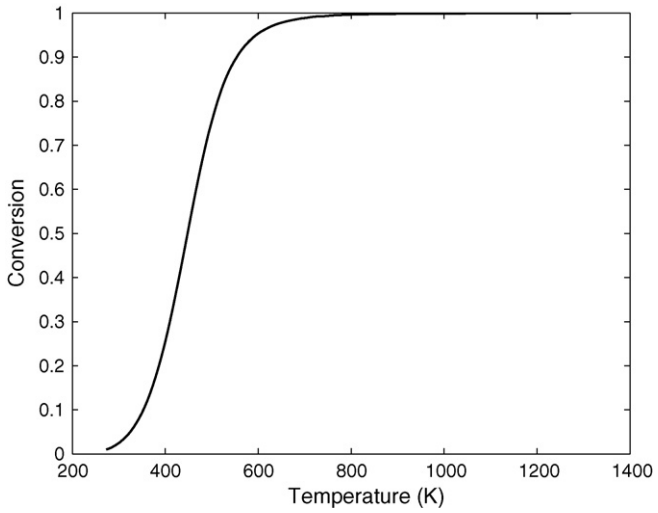

Fig. 3. Equilibrium conversion as a function of temperature.

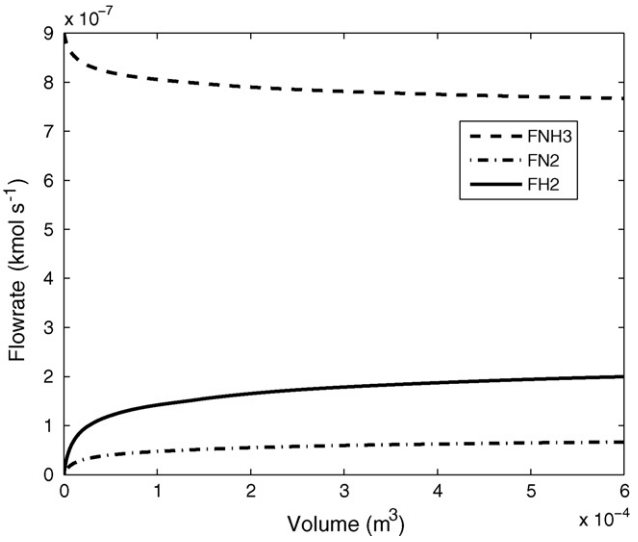

Fig. 4. Feed rate as a function of reactor volume under adiabatic conditions.

The mathematical model developed above provides a relation between ammonia flow rate into the reactor and hydrogen flow rate out of the reactor. The reactor temperature changes as a function of the reactor length depending on the heat flux provided to the reactor, which in turn affects conversion. There is a constraint that 100% conversion of ammonia is required to avoid poisoning the PEM fuel cell catalyst. Increasing the flow rate of ammonia increases the heat required to achieve complete conversion, which in turn requires more power to be generated by the fuel cell stack. Thus, it is necessary to choose the flow rate of ammonia into the reactor, the heat flux to the reactor and the size of the fuel cell stack to achieve optimal performance. These design parameters were set via trial-and-error by running a large number of simulations. The design equations described by Eqs. (3)–(11) were integrated numerically. The flow rate of ammonia entering the reactor was set at 0.0009 mol s^{-1}. Initial simulations were conducted to determine hydrogen production when the reactor was operated adiabatically. Fig. 4 shows the plot of flow rates of ammonia, hydrogen and nitrogen as a function of reactor volume when the inlet temperature is 793 K and the inlet pressure is 2 bar. It is observed that the conversion of ammonia is low. Fig. 5 shows the corresponding

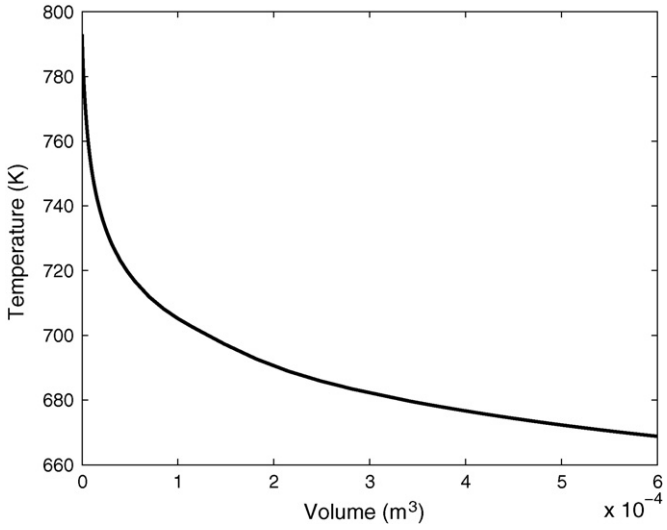

Fig. 5. Temperature as a function of reactor volume under adiabatic conditions.

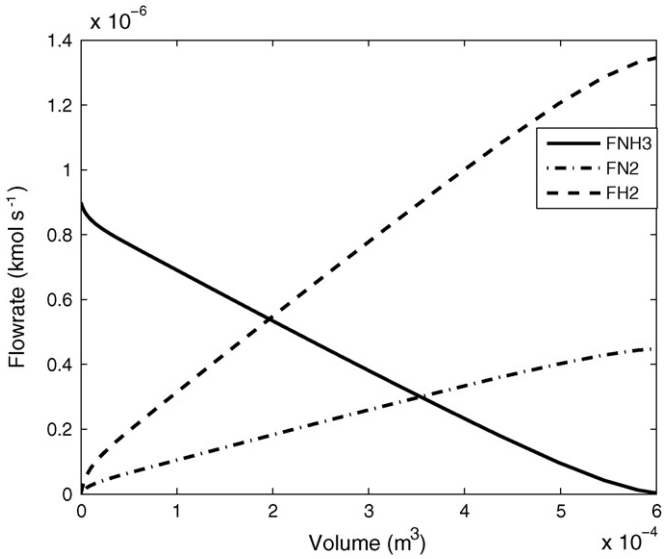

Fig. 6. Feed rate as a function of reactor volume when the reactor is heated electrically.

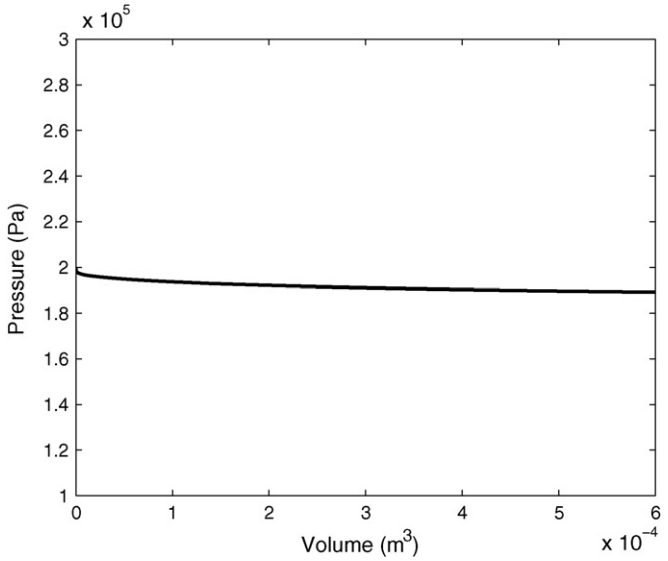

Fig. 8. Reactor pressure as a function of reactor volume.

temperature profile and it is observed that the temperature falls below 720 K at a reactor volume of 1.5×10^{-4} m and the reaction rate is almost zero below this temperature. This leads to the conclusion that adiabatic operation is impractical and it is necessary to provide an external source of heat.

Simulations were conducted assuming that there is a constant heat flux of 70 kJ m^{-3} s^{-1} to the reactor via electrical heating. This is equivalent of 42 W of power for the reactor and so sufficient hydrogen has to be generated to produce 142 W of power in the fuel cell, out of which 42 W is used for heating and the remaining 100 W is available for external use. Fig. 6 shows the plot of flow rates of ammonia, hydrogen and nitrogen as a function of reactor volume when the inlet temperature is 793 K and the inlet pressure is 2 bar. The flow rate of hydrogen coming out of the reactor is 1.35×10^{-3} mol s^{-1}. Fig. 7 shows the corresponding temperature profile and it is observed that while the temperature initially decreases due to the endothermic reaction, it starts to increase due to the supply of heat to the reactor, thereby increasing the reaction rate. Fig. 8 shows the corresponding pressure profile as a function of reactor volume. It is observed that the pressure drop is small (about 8%). This indicates that the pressure drop due to flow through the packed-bed is approximately balanced by the pressure increase due to increase in total moles due to the decomposition of ammonia to hydrogen.

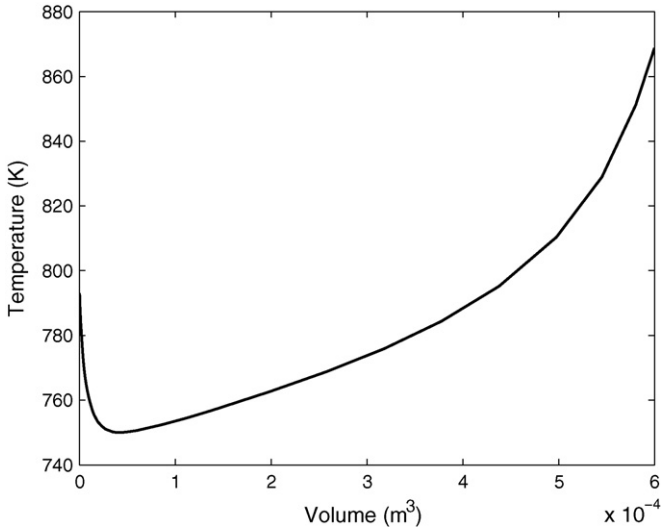

Fig. 7. Temperature as a function of reactor volume when the reactor is heated electrically.

Table 4
Adsorbent required for ammonia removal (2000 Wh operation).

Adsorbent	Weight required
6%	92 g
8%	69 g
10%	55 g

The reactor simulations utilize a number of parameters obtained from the literature that are listed in Tables 1–3. There could be errors in estimating these parameters, which in turn can affect the calculation of predicted hydrogen simulation. Several simulations were conducted assuming that the rate expressions were off by up to 20%. It was determined that the predicted hydrogen flow rate changed by less than 1% and so the model is relatively insensitive to errors in parameter estimation up to an overall error of 20% in the rate expressions.

The equilibrium calculation represented by Fig. 3 indicates that conversion of ammonia at an exit temperature of 870 K is in excess of 99.5%. If we assume the worst case scenario of 99.5% conversion, as much as 2500 ppm of ammonia may be present in the exit gas that goes to the fuel cell. It is necessary to reduce ammonia to *ppb* levels to avoid performance loss in the PEM fuel cell [17] and for this purpose an adsorbent is necessary. Commercially available adsorbents, such as Ammosorb (manufactured by Nucor, Inc.), can adsorb between 6 and 8% ammonia. Proprietary carbon adsorbents developed by MesoSystems Technology, Inc. can adsorb up to 10% ammonia by weight [18]. Table 4 shows the amount of adsorbent needed for reducing ammonia from 2500 ppm to less than 1 ppb for a 2000 Wh operation for three different adsorbents. This amount of adsorbent material can be easily incorporated in a practical device.

3. Fuel cell stack design

The relation between hydrogen flow rate, current, and the number of cells is given by Larminie and Dicks [19]:

$$I = \frac{2F\epsilon F_{H_2}}{n} \quad (12)$$

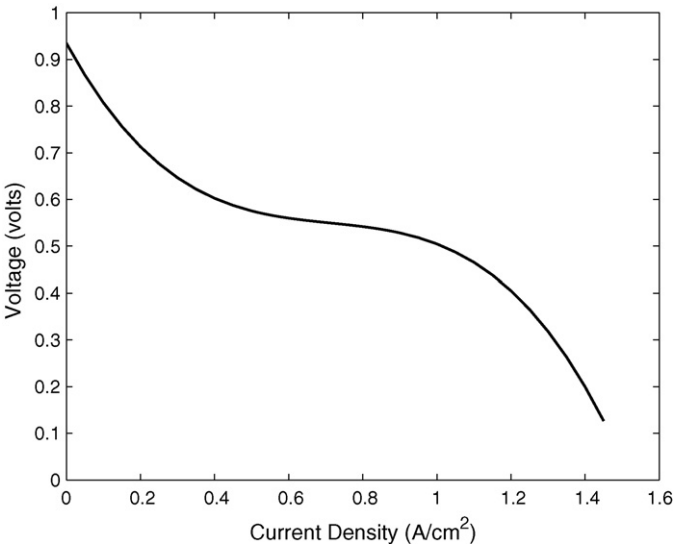

Fig. 9. Polarization curve.

Table 5
Fuel cell stack parameters.

Number of cells, n	20
Area of cross section of each cell, A	20.25 cm^2
Efficiency factor, ϵ	0.85
Faraday's constant, F	96,487 C mol^{-1}

where I is the current, F is the Faraday's constant, F_{H_2} is the molar flow rate of hydrogen entering the fuel cell stack, ϵ is an efficiency factor and n is the number of cells in the fuel cell stack.

The desired power generated by the fuel cell stack is computed from:

$$P = VIn \tag{13}$$

where P is the power and V is the voltage.

The polarization curve shown in Fig. 9 is utilized to model the relation between voltage and power density, which was developed from experimental data at 60 ° C by Chang et al. [20]. Using the above equations, an iterative calculation was performed to determine the number of cells that would produce 142 W of power. Fuel cell stack parameters are shown in Table 5. It was determined that using a stack with 20 cells resulted in a total current of 13 A, a total voltage of 11.92 V from the stack resulting in a total power of 142 W. The heat requirement for the reactor was previously determined to be 42 W. Thus, a net power of 100 W is generated.

The reactor exit gases are at 870 K while the fuel cell operates at 333 K. The excess heat can be used for vaporizing the water necessary for humidifying the hydrogen stream that goes into the fuel cell. The rate of enthalpy change of the reactor product stream from 870 to 333 K is 28.7 W while the energy required to humidify sufficient water to get 100% relative humidity in the fuel cell is less than 10 W. Thus, even if the heat transfer efficiency from the reactor exit gas to the vaporizor is 35%, there is sufficient heat to humidify the fuel cell inlet gas. Additional cooling of the reactor exit gas, if necessary, can be done via a heat sink. Alternatively, excess steam can be generated and vented.

4. Conclusions

In this paper, reaction engineering principles are utilized to analyze process conditions for producing sufficient hydrogen in an ammonia decomposition reactor to generate net power of 100 W in a PEM fuel cell stack. It is shown that operating the reformer adiabatically results in a sharp decrease in temperature due to endothermic reaction, which results in low conversion of ammonia. For this reason, the reactor is heated electrically and thus excess power needs to be generated by the fuel cell for this purpose. It is shown that a flow rate of 0.0009 mol s^{-1} of ammonia is required in conjunction with a fuel cell stack of 20 cells to produce 142 W of power, out of which 42 W is used to heat the reactor and the remaining 100 W is available for external use. This indicates an overall efficiency of 70%. There is an energy cost associated with producing ammonia, which is not accounted for in this calculation. This design is not suitable for large power plant applications in the megawatt range. With the requirement of utilizing 30% of the power generated for hydrogen production, this application is more suitable for small power applications in remote areas, such as rural farming communities, which are not connected to the power grid but have a ready source of ammonia. It is necessary to use an adsorbent column to reduce the ammonia in the reactor exit gas to less than 1 ppb. Our calculations indicate that less than 100 g of adsorbent is sufficient for a 2000 Wh operation. An energy balance on the reactor exit gas indicates that there is sufficient energy to vaporize the water necessary to humidify the hydrogen stream entering the PEM fuel cell.

Acknowledgement

Funding from the USA Foundation is gratefully acknowledged.

References

[1] H.W. Cooper, Fuel cells, the hydrogen economy and you, Chem. Eng. Prog. 103 (2007) 34–43.
[2] J.D. Holladay, J. Hu, D.L. King, Y. Wang, An overview of hydrogen production technologies, Catal. Today 139 (2009) 244–260.
[3] A.V. Pattekar, M.V. Kothare, A radial microfluidic fuel processor, J. Power Sources 147 (2005) 116–127.
[4] J.M. Sohn, Y.C. Byun, J.Y. Cho, J. Choe, K.H. Song, Development of the integrated methanol fuel processor using micro-channel patterned devices and its performance for steam reforming of methanol, Int. J. Hydrogen Energy 32 (2007) 5103–5108.
[5] O. Tan, E. Masalaci, Z.I. Onsan, A.K. Avci, Design of a methane processing system producing high-purity hydrogen, Int. J. Hydrogen Energy 33 (2008) 5516–5526.
[6] B. Lindstrom, J.A.J. Karlsson, P. Ekdunge, L. De Verdier, B. Haggendal, J. Dawody, M. Nilsson, L.J. Pettersson, Diesel fuel reformer for automotive fuel cell applications, Int. J. Hydrogen Energy 34 (2009) 3367–3381.
[7] H.S. Chu, F. Tsau, Y.Y. Yan, K.L. Hsueh, F.L. Chen, The development of a small PEMFC combined heat and power system, J. Power Sources 176 (2008) 499–514.
[8] G. Kolb, T. Baier, J. Schurer, D. Tiemann, A. Ziogas, H. Ehwald, P. Alphonse, A micro-structured 5 kW complete fuel processor for iso-octane as hydrogen supply system for mobile auxiliary power units: Part I. Development of autothermal reforming catalyst and reactor, Chem. Eng. J. 137 (2008) 653–663.
[9] A. Kundu, J.H. Jang, J.H. Gil, C.R. Jung, H.R. Lee, S.H. Kim, B. Ku, Y.S. Oh, Micro-fuel cells: Current development and applications, J. Power Sources 170 (2007) 67–78.
[10] K. Gardner, Portable Fuel Cells for Military Applications, Washington, DC, 2001.
[11] A. Wojcik, H. Middleton, I. Damopoulos, J. Van Herle, Ammonia as a fuel in solid oxide fuel cells, J. Power Sources 118 (2003) 342–348.
[12] M.R. Powell, M. Fountain, A.S. Chellappa, Compact fuel cell power supplies with safe fuel storage, in: Proceedings of the Army Science Conference, Orlando, FL, November, 2005.
[13] A.S. Chellappa, C.M. Fischer, W.J. Thomson, Ammonia decomposition kinetics over Ni-Pt/Al_2O_3 for PEM fuel cell applications, Appl. Catal. A: Gen. 227 (2002) 231–240.
[14] H.S. Fogler, Elements of Chemical Reactor Engineering, Prentice-Hall, Upper Saddle River, 2006.
[15] R.B. Bird, L.E. Stewart, E.N. Lightfoot, Transport Phenomena, 2nd ed., John Wiley and Sons, 2006.
[16] B.E. Poling, J.M. Prausnitz, J.P. O'Connell, The Properties of Gases and Liquids, 5th ed., McGraw-Hill, 2001.
[17] R. Halseid, P.J.S. Vie, R. Tunold, Effect of ammonia on the performance of polymer electrolyte membrane fuel cells, J. Power Sources 154 (2006) 343–350.
[18] A.S. Chellappa, M.R. Powell, M. Fountain, C.J. Call, N.A. Godshall, Compact fuel processors for PEM fuel cells, Adv. Hydrogen Energy Fuel Chem. Div. Preprints 47 (2002) 713–715.
[19] J. Larminie, A. Dicks, Fuel Cell Systems, Wiley, New York, 2000.
[20] H. Chang, J.R. Kim, J.H. Cho, H.K. Kim, K.H. Choi, Materials and processes for small fuel cells, Solid State Ion. 148 (2002) 601–606.